ARF-GEF cytohesin-2/ARNO regulates R-Ras and α5-integrin recycling through an EHD1-positive compartment

Joseph C. Salem, Marta M. Reviriego-Mendoza, and Lorraine C. Santy
Department of Biochemistry and Molecular Biology, Pennsylvania State University, University Park, PA 16802

ABSTRACT When expressed in epithelial cells, cytohesin-2/ARNO, a guanine nucleotide exchange factor (GEF) for ARF small GTPases, causes a robust migration response. Recent evidence suggests that cytohesin-2/ARNO acts downstream of small the GTPase R-Ras to promote spreading and migration. We hypothesized that cytohesin-2/ARNO could transmit R-Ras signals by regulating the recycling of R-Ras through ARF activation. We found that Eps15-homology domain 1 (EHD1), a protein that associates with the endocytic recycling compartment (ERC), colocalizes with active R-Ras in transiently expressed HeLa cells. In addition, we show that EHD1-positive recycling endosomes are a novel compartment for cytohesin-2/ARNO. Knockdown or expression of GEF-inactive (E156K) cytohesin-2/ARNO causes R-Ras to accumulate on recycling endosomes containing EHD1 and inhibits cell spreading. E156K-ARNO also causes a reduction in focal adhesion size and number. Finally, we demonstrate that R-Ras/ARNO signaling is required for recycling of α5-integrin and R-Ras to the plasma membrane. These data establish a role for cytohesin-2/ARNO as a regulator of R-Ras and integrin recycling and suggest that ARF-regulated trafficking of R-Ras is required for R-Ras–dependent effects on spreading and adhesion formation.

Monitoring Editor
Adam Linstedt
Carnegie Mellon University

Received: May 14, 2015
Revised: Sep 11, 2015
Accepted: Sep 11, 2015

INTRODUCTION

Epithelial cells normally form an immobile barrier that line organs and luminal space. However, they can become highly migratory during certain conditions, such as wound healing (Fenteany *et al.*, 2000; Santy and Casanova, 2001; Farooqui and Fenteany, 2005), developmental morphogenesis (Birchmeier *et al.*, 2003; Bryant and Mostov, 2008), and cancer metastasis (Thiery, 2002; Sabe, 2003). Epithelial cell migration is mediated in part by molecular switches called small GTPases (Ridley, 2001). Small GTPases bind guanine nucleotide and cycle between an active, GTP-bound state and an inactive, GDP-bound state. Accessory proteins called GTPase-activating proteins (GAPs) stimulate the GTPase to hydrolyze the bound GTP, and guanine nucleotide exchange factors (GEFs) displace bound GDP, allowing GTP to bind and activate the GTPase. In the GTP-bound state, small GTPases can associate with effector proteins to activate downstream pathways.

ADP-ribosylation factor (ARF) small GTPases are regulators of intracellular vesicular traffic. They mediate traffic by recruiting coat proteins and directly activating enzymes that modify membrane lipids (D'Souza-Schorey and Chavrier, 2006; Donaldson and Jackson, 2011). There are three classes of ARFs: class I ARFs (ARF1, ARF2, ARF3) and class II ARFs (ARF4, ARF5) regulate traffic near the Golgi. ARF6, the only member of the class III ARFs, regulates traffic near the plasma membrane. ARF6 is different from other ARF GTPases, in that its expression leads to reorganization of cortical actin (Song *et al.*, 1998; Radhakrishna *et al.*, 1999; Santy and Casanova, 2001; Palacios and D'Souza-Schorey, 2003). Of importance, ARF1 also functions near the periphery during dynamic plasma membrane events (Beemiller *et al.*, 2006; Cohen *et al.*, 2007).

Although several ARF-GEFs help regulate endocytosis and recycling, the cytohesin family of ARF GEFs is of particular interest because they are involved in altering cell shape, migration, and recycling of integrins (Frank *et al.*, 1998; Santy and Casanova, 2001;

This article was published online ahead of print in MBoC in Press (http://www.molbiolcell.org/cgi/doi/10.1091/mbc.E15-05-0278) on September 16, 2015.

Address correspondence to: Lorraine C. Santy (lcsanty@psu.edu).

Abbreviations used: ARF, ADP-ribosylation factor; ARNO, ADP-ribosylation factor nucleotide site opener; EHD1, Eps-15 homology domain–containing protein 1; GEF, guanine nucleotide exchange factor; GRP1, general receptor for phosphoinositides-1; RLIP76, Ral-interacting protein of 76 kDa.

Santy *et al.*, 2005; Casanova, 2007; Oh and Santy, 2010, 2012; Torii *et al.*, 2010; White *et al.*, 2010; Davies *et al.*, 2014). There are four members of the cytohesin family of ARF-GEFs. They all contain a N-terminal coiled-coil domain, a conserved catalytic Sec7 domain, a pleckstrin homology (PH) domain, and a short C-terminal polybasic domain (Casanova, 2007). The Sec7 domain contains a highly conserved and invariant glutamic acid that displaces bound GDP through repelling charges (Béraud-Dufour *et al.*, 1998; Mossessova *et al.*, 1998).

Cytohesin-2/ADP-ribosylation factor nucleotide site opener (ARNO) is a robust activator of ARF6 when overexpressed and causes cells to migrate in culture through downstream activation of Rac1 (Santy and Casanova, 2001; Santy *et al.*, 2005). Cytohesin-2/ARNO is also required for β1-integrin recycling (Oh and Santy, 2010, 2012). Disrupting integrin recycling has negative effects on cell migration (Powelka *et al.*, 2004; Tayeb *et al.*, 2005; Oh and Santy, 2010, 2012). The N-terminal coiled-coil domain of cytohesin-2/ARNO serves two functions: it acts as an autoinhibitor of cytohesin-2/ARNO function (Hiester and Santy, 2013) and as a scaffold by promoting the assembly a multiprotein complex containing scaffolding proteins GRASP and CNK3/IPCEF1 and the Rac-GEF DOCK180/Elmo (White *et al.*, 2010; Attar *et al.*, 2012; Attar and Santy, 2013). Therefore, by activating ARF6 and forming a complex with DOCK180/Elmo, cytohesin-2/ARNO promotes downstream activation of Rac1 and cell migration.

R-Ras is more distantly related to better-known members of the Ras family (H-, K-, N-Ras; Lowe and Goeddel, 1987). R-Ras promotes cell spreading, adhesion formation, plasma membrane ruffling, and integrin activation (Furuhjelm and Peränen, 2003; Kwong *et al.*, 2003; Holly *et al.*, 2005; Jeong *et al.*, 2005; Wozniak *et al.*, 2005; Conklin *et al.*, 2010; Sandri *et al.*, 2012). R-Ras is mainly expressed in vascular tissue (Komatsu and Ruoslahti, 2005) but has been shown to be critical for adhesion and migration in fibroblasts and epithelial cells in culture. Although specific mutations in R-Ras have not been associated with cancer, R-Ras has been found to be up-regulated in cervical cancer (Gao *et al.*, 2014), gastric cancers (Nishigaki *et al.*, 2005), prostate cancer (Wong *et al.*, 2007), and gliomas (Nakada *et al.*, 2005). The importance of R-Ras in migration has been demonstrated across multiple cell types, including skeletal myoblast (Suzuki *et al.*, 2000), myeloid (Holly *et al.*, 2005), endothelial (Sandri *et al.*, 2012), fibroblast (Goldfinger, 2006), and epithelial (Keely *et al.*, 1999; Furuhjelm and Peränen, 2003; Rincón-Arano *et al.*, 2003; Jeong *et al.*, 2005; McHugh *et al.*, 2010).

Recent evidence suggests that cytohesin-2/ARNO and small the GTPase R-Ras function in the same signaling pathway to promote cell migration (Goldfinger, 2006; Lee *et al.*, 2014; Mott and Owen, 2014). Overexpression of constitutively active (38V) R-Ras causes a scattering phenotype in Madin–Darby canine kidney (MDCK) cells that is very similar to that in cells expressing cytohesin-2/ARNO (Khwaja *et al.*, 1998; Santy and Casanova, 2001). R-Ras also has been shown to feed into the activation of Rac1 (Goldfinger, 2006; Sandri *et al.*, 2012; Lee *et al.*, 2014). A unique R-Ras effector, Ral-interacting protein of 76 kDa (RLIP76), associates with cytohesin-2/ARNO (Goldfinger, 2006), and this interaction is required for ARF6 activation and migration (Lee *et al.*, 2014). However, a precise mechanism of how R-Ras enhances cell spreading through integrin regulation is not clear. Rather than directly promoting integrin activation, as was once suggested (Zhang *et al.*, 1996), much of the early data show an indirect mechanism by which R-Ras inhibits integrin suppression mediated by H-Ras (Hughes *et al.*, 1997; Ramos *et al.*, 1998; Sethi *et al.*, 1999; Hughes *et al.*, 2002). Others have shown that R-Ras does not directly change the binding affinity of integrins (Kwong *et al.*, 2003) and does not increase the total amount of cell surface integrin (Zhang *et al.*, 1996; Rincón-Arano *et al.*, 2003; Sandri *et al.*, 2012). One way in which R-Ras could promote integrin activation is by regulating the recycling of integrins from internal compartments to the periphery (Takaya *et al.*, 2007). β1-Integrin recycles using many Rab small GTPases, including Rab21 (Pellinen *et al.*, 2006), Rab11 (Powelka *et al.*, 2004), Rab8 (Hattula *et al.*, 2006), Rab4 (Roberts *et al.*, 2001), and Rab25 (Caswell *et al.*, 2007), as well as ARF6 (Powelka *et al.*, 2004) and Eps-15 homology domain–containing protein 1 (EHD1; Jović *et al.*, 2007).

It is clear that as a regulator of integrin function, R-Ras could recycle within a similar compartment as integrins. A distinct population of R-Ras that localizes at the peripheral plasma membrane promotes the clustering and eventual endocytosis of β1-integrin in COS-7 cells (Conklin *et al.*, 2010). In endothelial cells, R-Ras, Rab5, and Rab5-adaptor RIN2 escort integrins bound to extracellular matrix to early endosomes (Sandri *et al.*, 2012). R-Ras has been shown to traffic using Rab11 (Conklin *et al.*, 2010; Wurtzel *et al.*, 2012), and posttranslational lipid modifications are critical for proper sorting and recycling of R-Ras (Wurtzel *et al.*, 2012). Furthermore, endogenous R-Ras has been described to be in tubular-like compartments in NIH-3T3 fibroblasts (Wurtzel *et al.*, 2012).

Given evidence that that R-Ras, cytohesin-2/ARNO, and ARF6 function in a similar pathway to promote migration and integrin recycling, we wondered whether cytohesin-2/ARNO could direct trafficking of R-Ras and integrin from an internal compartment to the plasma membrane.

RESULTS

The GEF-activity of cytohesin-2/ARNO affects the morphology of EHD1-positive recycling endosomes

At the start of endocytosis, peripheral ARFs (i.e., ARF6 and ARF1) are activated at the plasma membrane and are subsequently inactivated before merging with endosomes (Donaldson *et al.*, 2009; Grant and Donaldson, 2009). When cargo is ready to exit recycling endosomes and traffic back out to the plasma membrane, ARFs are again activated, allowing vesicles to bud off and recycle back out to the plasma membrane. EHD1 associates with preexisting tubular membrane of the endocytic recycling compartment (ERC). EHD1-positive recycling endosomes are also enriched with ARF6 (Caplan *et al.*, 2002). The ERC is particularly easy to visualize in HeLa cells expressing EHD1, as they form distinct tubular structures. When we plated HeLa cells on fibronectin matrix and allowed them to express Cerulean-EHD1, cells formed mostly small, punctate EHD1 endosomes and individual tubes that extend radially from the perinucleus (Figure 1A). In contrast, cells expressing wild-type (WT) cytohesin-2/ARNO showed almost exclusively punctate EHD1 endosomes with very limited elongated tubular structure. A population of EHD1 was seen at the periphery of cells at sites enriched with mCherry WT-ARNO (Figure 1B). In contrast to both EHD1 and EHD1/WT-ARNO–transfected cells, HeLa cells expressing GEF-inactive (E156K) cytohesin-2/ARNO were noticeably less spread and showed more intracellular EHD1 in the form dense, perinuclear accumulation or as extensive tubular formations that could extend through the entire length of the cell (Figure 1C). These data suggest that if cytohesin-2/ARNO–induced ARF activation is blocked, EHD1-positive vesicles will no longer be able to properly recycle, causing an accumulation of cargo in the ERC.

If cytohesin-2/ARNO regulates recycling from EHD1 endosomes and activates ARFs there, we should be able to visualize membrane-bound cytohesin-2/ARNO on EHD1-positive endosomes.

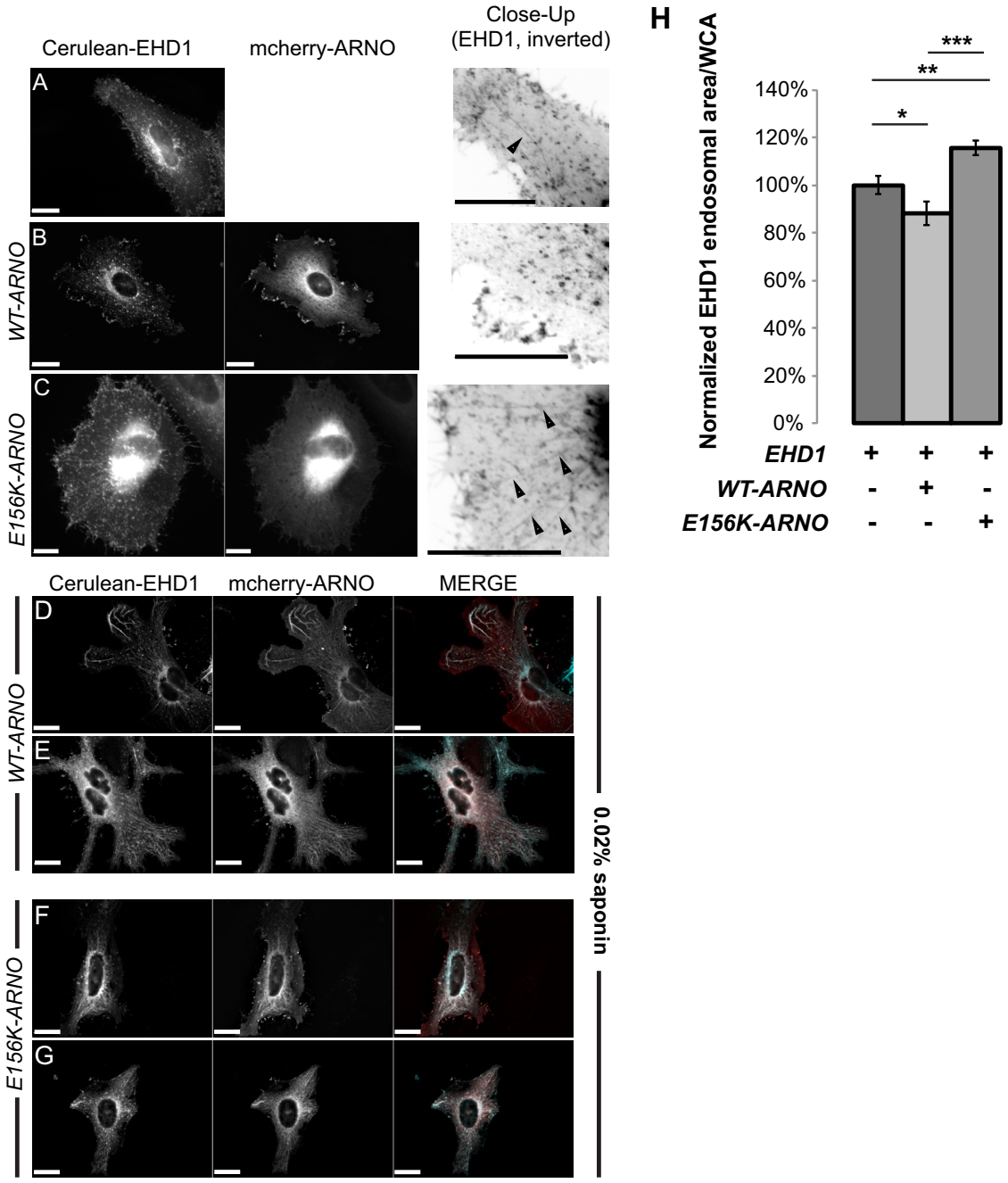

FIGURE 1: Cytohesin-2/ARNO colocalizes with EHD1-positive endosomes and affects their morphology. (A–C) HeLa cells were transfected using Neon electroporation and allowed to express overnight. The next day, cells were treated with 0% saponin permeabilization buffer and fixed and imaged. Black arrows show EHD1 tubules. (D–G) HeLa cells were transfected as described for A–C. Before fixation, cells were permeabilized with 0.02% saponin for 1 min, washed quickly with PBS, and then fixed. In the merged image, EHD1 is pseudocolored cyan and ARNO is red. (H) Cells treated in A–C were masked for whole-cell area using SlideBook 6.0 software. A 2D Laplacian filter was applied to the EHD1 channel and subsequently masked. The endosomal area was measured, and the ratio of endosomal area per whole-cell area was graphed. Images underwent deconvolution using SlideBook 6.0 (EHD1, 47 cells; EHD1/WT-ARNO, 32 cells; EHD1/E156K, 76 cells). Samples were analyzed from two independent experiments using a two-sample *t* test using MiniTab 17. ***$p < 0.001$, **$p < 0.01$, *$p < 0.05$. Scale bars, 20 μm.

Cytohesin-2/ARNO is mostly cytosolic, and initial coexpression of Cerulean-EHD1 and mCherry-ARNO did not clearly resolve colocalization on EHD1 endosomes. Overall EHD1 and cytohesin-2/ARNO (WT and E156K) showed high colocalization (Supplemental Table S1). To resolve cytohesin-2/ARNO-EHD1 colocalization at tubular endosomes, we allowed cytosolic cytohesin-2/ARNO to leak out by permeabilizing cells using saponin before fixation. In saponin-treated cells, both WT-ARNO (Figure 1, D and E) and E156K-ARNO (Figure 1, F and G) showed high colocalization (Supplemental Table S1) of cytohesin-2/ARNO with EHD1 on tubular endosomes. Of interest, in cells in which Cerulean-EHD1 was expressed alone, saponin concentrations of 0.02% led to complete

loss of EHD1 in most cells (Supplemental Figure S1A). Cells treated with 0.02% saponin that were able to retain EHD1 showed a much more diffusely distributed EHD1. These data confirm a previous finding showing EHD1 sensitivity to digitonin permeabilization (Cai *et al.*, 2013) and suggest that cytohesin-2/ARNO may aid in stabilizing EHD1 on the membrane. Taken together, these data suggest a previously unknown role for cytohesin-2/ARNO in regulating recycling at the ERC.

Because E156K-ARNO expression increases intracellular accumulation of EHD1, we sought to measure this accumulation using microscopy and masking techniques. We applied a two dimensional (2D) Laplacian filter to the EHD1 channel, which allowed us to resolve EHD1 endosomes throughout all areas of the cell. We masked these EHD1 endosomes and asked which samples had more EHD1 endosomal area (μm^2) per whole-cell area ($\mu m^2/\mu m^2$). We noticed that HeLa cells expressing E156K-ARNO had significantly more EHD1 area per whole-cell area than the other samples (Figure 1H). Of importance, raw endosomal area did not differ greatly from each sample when whole-cell area was not considered (Supplemental Figure S1B). Although we did see more EHD1 endosomal area in WT-ARNO cells compared with E156K-ARNO cells ($p = 0.022$), this is not surprising, considering that cells on average are ~50% more spread. Taken together, these data demonstrate that cytohesin-2/ARNO colocalizes with ERC marker EHD1 and GEF activity of cytohesin-2/ARNO can affect the morphology of EHD1 recycling endosomes.

Wild-type, constitutively active (38V), but not dominant-negative (43N), R-Ras colocalizes with EHD1 tubular endosomes

Colocalization of R-Ras with recycling endosomal markers (i.e., Rab11) has been widely reported (Conklin *et al.*, 2010; Takaya *et al.*, 2007; Wurtzel *et al.*, 2012), and EHD1 has been associated with β1-integrin recycling and cell spreading (Jović *et al.*, 2007). To our knowledge, no one has investigated whether R-Ras associates with EHD1-positive endosomes. Although HeLa cells express R-Ras endogenously (Furuhjelm and Peränen, 2003), immunofluorescence staining of endogenous R-Ras has been mostly uninformative. Therefore we began by transiently coexpressing mCherry-tagged WT, constitutively active (38V), and dominant-negative (43N) R-Ras with Cerulean-EHD1 in HeLa cells plated on fibronectin. WT and 38V R-Ras colocalized (Supplemental Table S2) with EHD1 tubules and peripheral pools of plasma membrane EHD1 (Figure 2, A and B). EHD1 tubular endosomes, particularly in 38V-expressing cells, had a beaded or fragmented appearance. Despite sharing a similar colocalization value, the bulk of 43N R-Ras was noticeably absent from EHD1 tubules (Figure 2C). Occasionally EHD1 appeared as doughnut-shaped structures surrounding 43N R-Ras puncta. HeLa cells coexpressing EHD1 and 43N R-Ras still showed tubule formation, and average tubule length did not vary significantly among cells coexpressing EHD1 with WT, 38V, or 43N R-Ras (Supplemental Figure S2). Although it is unclear what these doughnut-shaped EHD1/43N R-Ras structures are, this is the most significant level of colocalization that 43N R-Ras has had with any endosomal marker. These data suggest that activation of R-Ras is required for its association with EHD1-positive tubules and not for formation of tubular endosomes per se, at least in cells overexpressing EHD1.

To characterize further the R-Ras trafficking itinerary, we coexpressed EHD1 and R-Ras with Rab8a and Rab11a, which are small GTPases involved in recycling. Because Rab8a and EHD1 are intimately associated in the formation of the ERC (Roland *et al.*, 2007; Sharma *et al.*, 2009), we hypothesized that R-Ras should also be

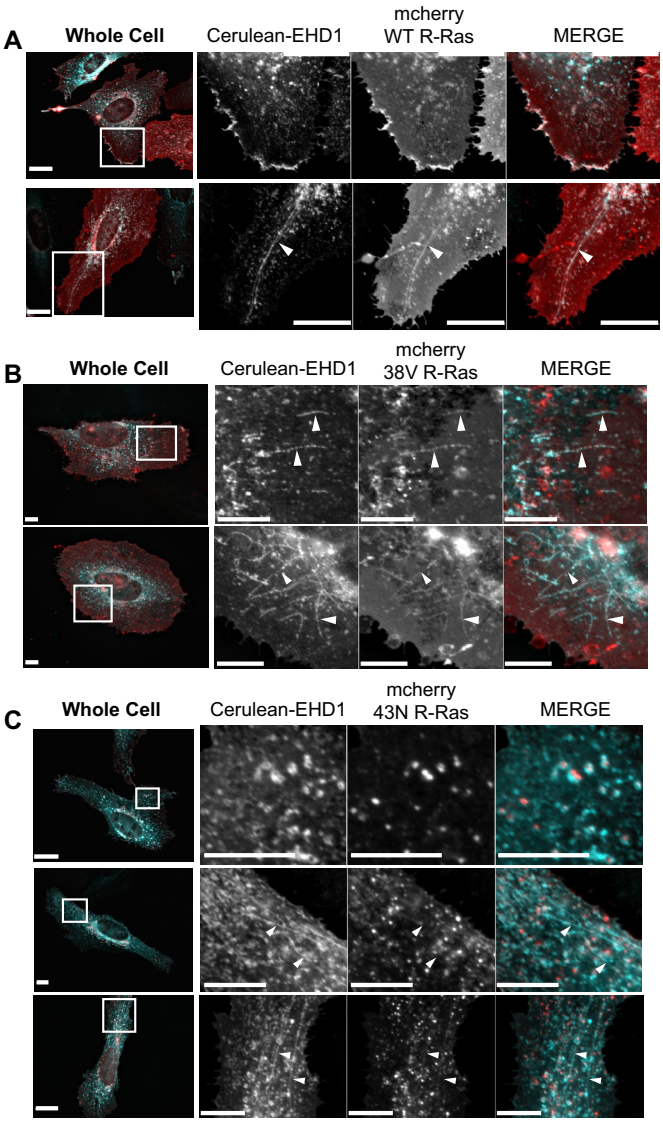

FIGURE 2: EHD1-positive recycling endosomes are compartments for active R-Ras. (A–C) HeLa cells were Neon transfected using Cerulean-EHD1 or mCherry WT R-Ras (A), constitutively active mCherry 38V R-Ras (B), or dominant-negative mCherry 43N R-Ras (C). Cells were allowed to express overnight on fibronectin-coated coverslips. The next day, cells were fixed and imaged using wide-field microscopy. White boxes on whole-cell images show representative cropped regions. Whereas WT and 38V R-Ras localize to EHD1 tubules, the bulk of 43N R-Ras is not with EHD1 tubules. Instead, EHD1 surrounds 43N R-Ras. White arrowheads show tubules. In the merged images, EHD1 is pseudocolored cyan and R-Ras is red. Images were deconvolved using SlideBook 6.0. Scale bars, 20 μm.

associated with Rab8a. Indeed, Rab8a colocalized with 38V R-Ras (Supplemental Figure S3A) on EHD1 tubules and at the peripheral plasma membrane (Supplemental Figure S3, B and C). However, 43N R-Ras did not colocalize with Rab8a or Rab11a and did not form similar doughnut structures with Rabs as we saw with EHD1 (Supplemental Figure S3, D, E, I, and J). Constitutively active R-Ras partially localized with Rab11a (Supplemental Figure S3F) on tubular endosomes but not at the plasma membrane (Supplemental Figure S3, G and H). Therefore R-Ras has a stronger association to EHD1/Rab8a than Rab11a. These findings show that R-Ras traffics through

an EHD1-positive ERC and that activation of R-Ras is required for its proper trafficking through EHD1 endosomes.

E156K-ARNO–expressing cells show an accumulation of 38V R-Ras at EHD1-positive endosomes

Because our data show that cytohesin-2/ARNO colocalizes and affects the morphology of EHD1-positive endosomes, we wondered whether we could trap R-Ras at EHD1 endosomes by specifically abrogating the GEF activity of cytohesin-2/ARNO. We reasoned that the GEF-activity of cytohesin-2/ARNO could promote R-Ras dependent spreading by 1) activating ARF at the plasma membrane and regulating endocytosis of R-Ras or 2) activating ARF on EHD1 endosomes, which would promote recycling to the plasma membrane. If cytohesin-2/ARNO is regulating endocytosis, we should see the bulk of R-Ras stuck at the plasma membrane if GEF-activity is destroyed. If cytohesin-2/ARNO–induced ARF activation is required for R-Ras recycling, we should see high levels of intracellular R-Ras, perhaps trapped on EHD1 recycling endosomes. HeLa cells expressing Venus 38V R-Ras with WT mCherry-ARNO and Cerulean-EHD1 showed punctate EHD1 distribution, with all three proteins enriched at the peripheral plasma membrane (Figure 3, A and B). In contrast, cells with mCherry E156K-ARNO showed intracellular accumulation of 38V R-Ras on EHD1-positive endosomes (Figure 3, C and D). In many cases, these endosomes were long tubes, on average ~2.5 times the length of EHD1 endosomes found in cells expressing WT-ARNO (Supplemental Figure S4). These data show that even in the presence of a constitutive upstream R-Ras signal, active R-Ras requires a functional cytohesin-2/ARNO for proper recycling and localization to the peripheral plasma membrane.

Knockdown of cytohesin-2/ARNO causes intracellular accumulation of R-Ras and EHD1

We reasoned that if destroying the GEF function of cytohesin-2/ARNO prevents ARF-induced recycling of components on the ERC, then knockdown of cytohesin-2/ARNO should mimic the effects of E156K-ARNO. In an endogenous cytohesin-2/ARNO background, overexpression of EHD1 alone results in significant tubule formation. However, there is a dramatic difference in EHD1 morphology among cells in which WT-ARNO is expressed versus GEF-inactive ARNO. Therefore we wondered whether reducing endogenous cytohesin-2/ARNO could cause a build-up effect in cells expressing EHD1 and R-Ras. To this end, we transfected HeLa cells with universal control small interfering RNA (siRNA) or siRNA targeting human cytohesin-2/ARNO. The next day, recovered cells were cotransfected using Cerulean-EHD1 and Venus R-Ras, and they were allowed to express overnight. We were able to reduce endogenous cytohesin-2/ARNO levels by 75% without altering the levels of cytohesin-3/general receptor for phosphoinositides-1 (GRP1), another ubiquitously expressed cytohesin (Supplemental Figure S5A). When we imaged HeLa cells coexpressing WT or 38V R-Ras with EHD1, we found that control cells showed EHD1 and R-Ras distributed in small, punctate endosomes or small, tubular endosomes (Figure 4, A and D). In contrast, knockdown of cytohesin-2/ARNO led to perinuclear accumulation of R-Ras and EHD1 (Figure 4, B and E). Particularly in 38V R-Ras–expressing cells, tube formation was so extensive that individual tubules were difficult to visualize. To measure intracellular accumulation, we applied the same masking techniques used previously. We again found significantly higher levels of endosomal area per whole-cell area of both

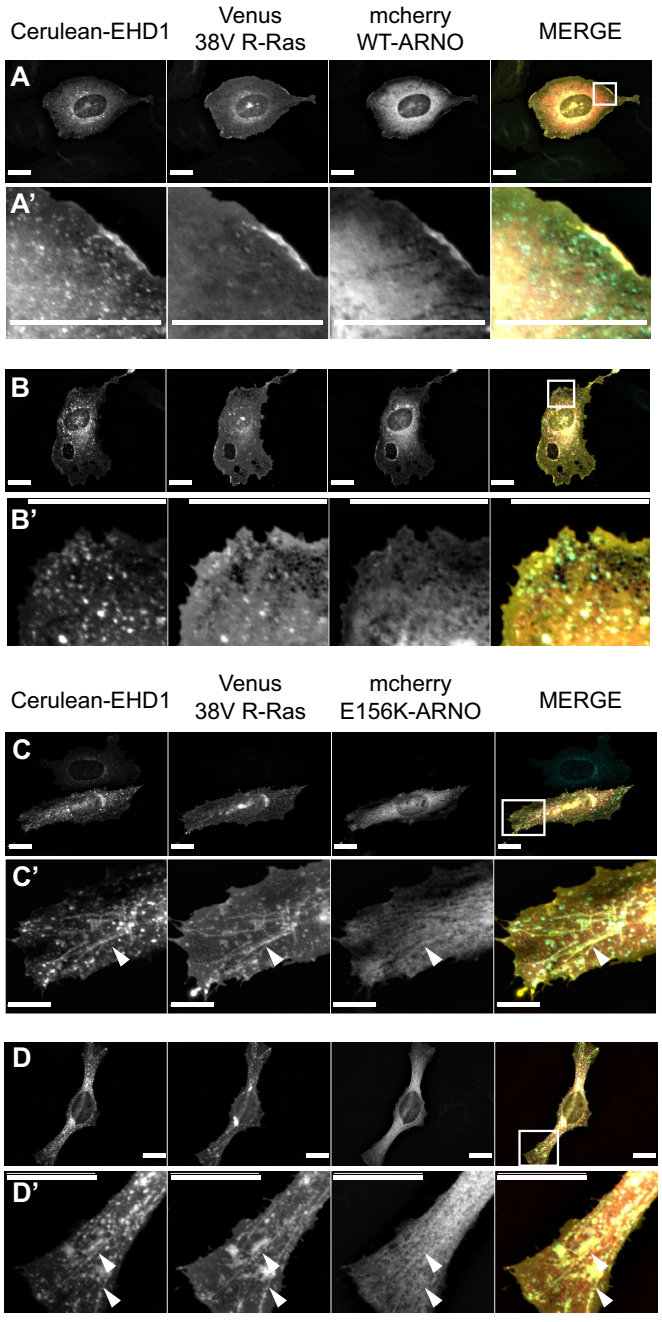

FIGURE 3: GEF-inactive E156K-ARNO causes an accumulation of 38V R-Ras on EHD1-positive endosomes. (A–D) HeLa cells were transiently transfected using Neon electroporation and allowed to express overnight on fibronectin-coated coverslips. Cerulean-EHD1, Venus 38V R-Ras, and either mCherry WT-ARNO (A, A′, B, B′) or GEF-inactive mCherry E156K-ARNO (C, C′, D, D′) were used for transfection. Cells were imaged as previously described. Expression of WT-ARNO distributed EHD1 and 38V R-Ras along the peripheral plasma membrane (A′), and 38V R-Ras was seen in small, EHD1-positive endosomes (B′). Expression of E156K-ARNO caused an accumulation of 38V R-Ras on long EHD1 tubules, away from the periphery (C′, D′). Whole-cell views are shown in A–D, where white boxes represent regions of interest shown in A′–D′. White arrows show tubules. In the merged images, EHD1 is pseudocolored cyan, R-Ras is yellow, and ARNO is red. Scale bars, 20 μm.

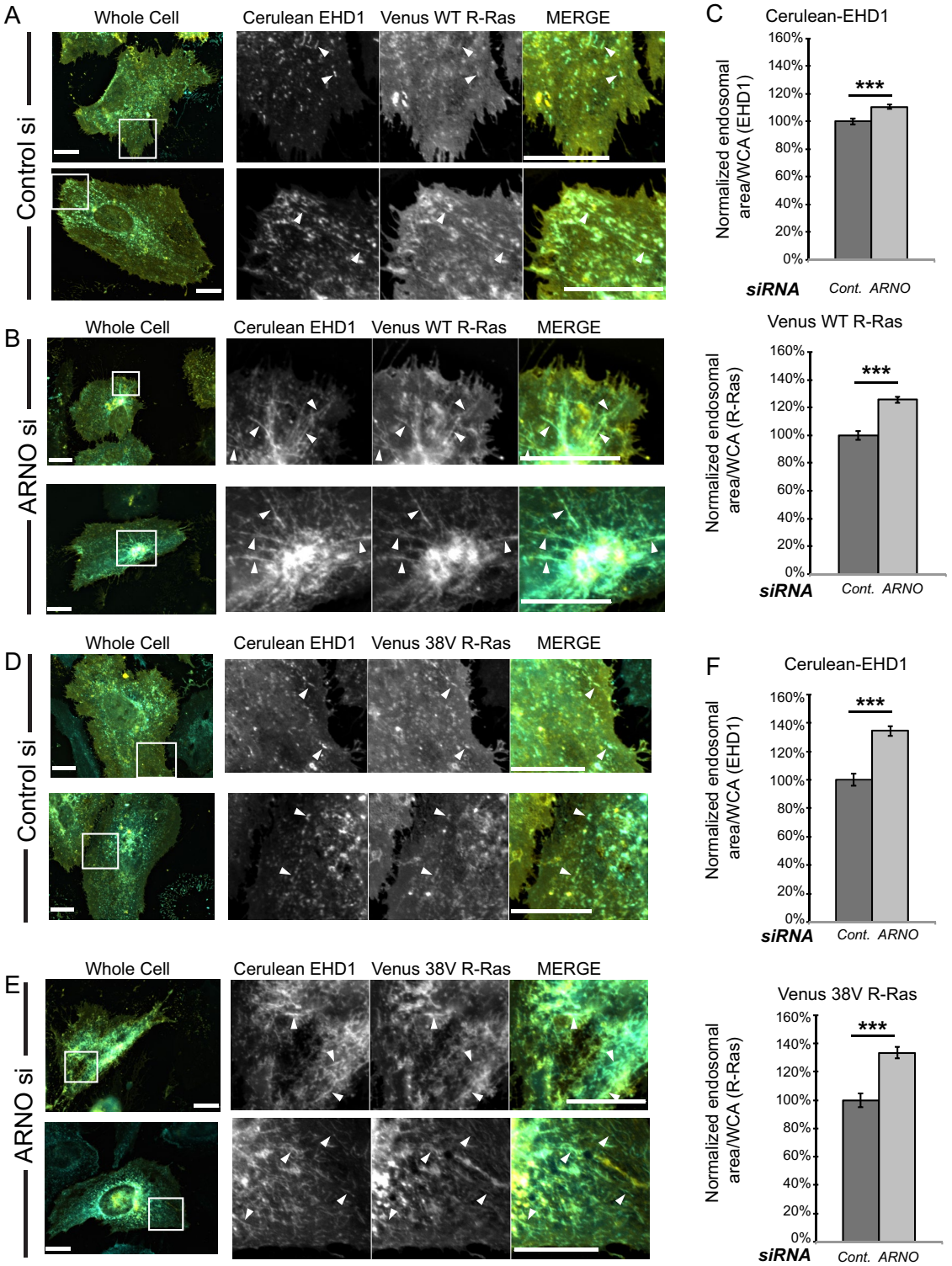

FIGURE 4: Knockdown of cytohesin-2/ARNO causes internal accumulation of EHD1 and R-Ras. Negative control siRNA (Invitrogen) or siRNA targeting human ARNO was transfected into HeLa cells using Neon electroporation. The next day, cells were transfected using Lipofectamine3000 (Life Technologies) with Cerulean-EHD1 and Venus WT R-Ras (A, B) or Venus 38V R-Ras (D, E) and allowed to express overnight to achieve 48 h of knockdown. Cells were fixed and imaged as previously described. We applied 2DLaplacian filtering to raw images to resolve endosomes using SlideBook 6.0 software. Filtered channels were masked for endosomal area, and nonfiltered channels were masked for whole-cell area. Normalized endosomal area per whole-cell area is shown (C, F). The following numbers of cells from one experiment were analyzed: 134 for EHD1/WT R-Ras control and ARNOsi and 140 for EHD1/38V R-Ras control and ARNOsi. Samples were analyzed using a two-sample *t* test using MiniTab 17. ***$p < 0.001$. Scale bars, 20 μm.

EHD1 and R-Ras (Figure 4, C and F). Cells expressing 38V R-Ras showed higher accumulation of EHD1 and R-Ras where cytohesin-2/ARNO levels were reduced. It is possible that 38V R-Ras traffics faster onto tubular compartments at a higher rate than WT R-Ras, causing a more noticeable build-up over time. We hypothesized that because 43N R-Ras was unable to associate with EHD1-positive endosomes, cytohesin-2/ARNO knockdown should have no effect on its intracellular accumulation. When we measured 43N R-Ras accumulation, there was no significant difference between control and cytohesin-2/ARNO–knockdown cells (Supplemental Figure S5B, right graph). Of interest, cytohesin-2/ARNO knockdown still caused extensive EHD1 accumulation in cells expressing 43N R-Ras (Supplemental Figure S5, C and D). These data suggest that cytohesin-2/ARNO knockdown only inhibits trafficking of R-Ras that can arrive at the ERC.

We noticed that increased intracellular accumulation of EHD1 as a result of cytohesin-2/ARNO knockdown manifests as enhanced tubule formation. Although our masks were able to measure total EHD1 accumulation, we wanted confirm that cytohesin-2/ARNO siRNA-treated cells contained more endosomes of larger size. To this end, we extracted morphometry parameters for endosomal perimeter and major axis length from our EHD1 masks. For each image analyzed, we calculated the percentage of endosomes that were within a certain micrometer range. Consistently, cytohesin-2/ARNO knockdown caused an increase in the percentage of endosomes with large (>10 μm) perimeter and large major axis length (>8 μm; Supplemental Table S3). Control cells typically contained higher percentages of smaller endosomes than knockdown cells. These data show that cytohesin-2/ARNO knockdown increases levels of intracellular EHD1/R-Ras on tubular endosomes.

As performed similarly for the double-transfectant cells, we analyzed single transfectants (expressing solely EHD1 or R-Ras). We saw an increase in intracellular EHD1, WT, and 38V R-Ras (Supplemental Figure S6, A, D, and G). Consistent with what was observed with the double transfectants, levels of intracellular 43N R-Ras did not change (Supplemental Figure S6J). Endosomal-like structures containing Venus WT or 38V R-Ras occasionally displayed a tubular morphology strikingly similar to the ERC when expressed alone without EHD1 (Supplemental Figure S6, E and H). In agreement with our previous observations, expression of Venus 43N-R-Ras was never found in tubular endosomes and displayed its typical, punctate, and highly intracellular morphology in control and cytohesin-2/ARNO–knockdown cells (Supplemental Figure S6, K and L). These data support the idea that cytohesin-2/ARNO is required for R-Ras recycling from the ERC.

Intracellular accumulation of both EHD1 and R-Ras corresponds to a reduction of short- and long-term cell spreading

If disrupting the GEF activity of cytohesin-2/ARNO inhibits R-Ras recycling and prevents its localization to the plasma membrane, then R-Ras–dependent effects on cell spreading should be inhibited. We returned to previous experiments and measured the whole-cell area of cells transfected with Cerulean-EHD1 or in combination with cytohesin-2/ARNO from Figure 1. We found that WT cytohesin-2/ARNO enhanced spreading of HeLa cells plated on fibronectin-coated coverslips compared with both EHD1- and EHD1/E156K-expressing cells (Figure 5A). Even when allowed to spread overnight in an endogenous cytohesin-2/ARNO background, E156K-ARNO still inhibited cells from spreading to levels of EHD1-expressing cells. We observed a similar effect on long-term cell spreading in cells in which we saw 38V R-Ras trapped with EHD1 (Figure 5B). Finally, we asked whether cytohesin-2/ARNO knockdown could also reduce cell spreading in actively spreading HeLa cells even when R-Ras is overexpressed. We transfected HeLa cells with Turquoise LifeAct or Venus 38V R-Ras alone. We then inhibited cytohesin-2/ARNO using siRNA-mediated knockdown, expression of E156K-ARNO, or pharmacologically, using SecinH3 (Hafner *et al.*, 2006). Cells were nonenzymatically harvested, seeded onto fibronectin-coated coverslips, and allowed to spread for 35 min before fixation. Cells transfected with siRNA targeting cytohesin-2/ARNO (80% knockdown; Supplemental Figure S7) showed a drastic reduction in cell area in both LifeAct and 38V R-Ras–expressing cells (Figure 5C). Spreading was reduced to levels comparable to cytohesin-2/ARNO knockdown whether cells were treated with SecinH3 or cotransfected with E156K-ARNO. In 38V-expressing cells, in which cytohesin-2/ARNO was inhibited, we noticed that despite adhering more quickly than cells expressing LifeAct, they ultimately failed to spread. In these cells, 38V R-Ras was highly accumulated near the center of spreading cells away from the periphery in punctate-to-tubular structures (Figure 5D). In cells treated with control siRNA, 38V R-Ras was found at the outer cell edges in typical ruffle-like structures. Our data suggest that a functional cytohesin-2/ARNO is required for a full spreading response in HeLa cells.

To show directly that R-Ras is required for cell spreading, we measured how well HeLa cells could spread on fibronectin in cells in which R-Ras was knocked down. R-Ras siRNA– treated cells showed a significant reduction in short-term cell spreading in cells expressing LifeAct (Figure 5E). We then tested the ability of cytohesin-2/ARNO overexpression to rescue spreading in R-Ras siRNA–treated cells. Cytohesin-2/ARNO overexpression was not able to enhance cell spreading in cells in which R-Ras levels were reduced. Taken together, these data demonstrate that both cytohesin-2/ARNO and R-Ras are required for cell spreading in HeLa cells.

E156K cytohesin-2/ARNO reduces focal adhesion size in HeLa cells

R-Ras has cell type–specific effects on focal adhesion formation. In HeLa cells, focal adhesions are sites for active R-Ras, and R-Ras is required for focal adhesion formation (Furuhjelm and Peränen, 2003). Dominant negative (43N) R-Ras does not localize with focal adhesions and reduces the size of focal adhesions in HeLa cells when it is expressed. A reduction in focal adhesion size suggests that integrin and/or R-Ras is not being trafficked to specific sites of need to established cell-ECM contacts. We reasoned that the GEF activity of cytohesin-2/ARNO would be required to properly localize R-Ras and therefore would phenocopy effects that expression of 43N R-Ras has on focal adhesions (Furuhjelm and Peränen, 2003). When we transfected HeLa cells with mCherry E156K-ARNO and stained for endogenous β1-integrin, cells showed significantly smaller focal adhesions than with LifeAct control cells or WT-ARNO–expressing cells (Figure 6A). In addition, the overall number of focal adhesions per cell decreased in cells expressing E156K-ARNO (Figure 6B). Control HeLa cells expressing Turquoise LifeAct to label F-actin showed large focal adhesions throughout the entire cell (Figure 6C). In contrast, E156K-ARNO cells had a noticeable absence of ventral adhesions and smaller peripheral adhesions (Figure 6D), very similar to what was reported with 43N R-Ras in HeLa cells (Furuhjelm and Peränen, 2003). Cells expressing WT cytohesin-2/ARNO could still produce large focal adhesions but also had a distinct population of β1-integrin all along the cell periphery (Figure 6E). We also saw a statistically significant ($p = 0.047$) reduction in the number of focal adhesions compared with control cells.

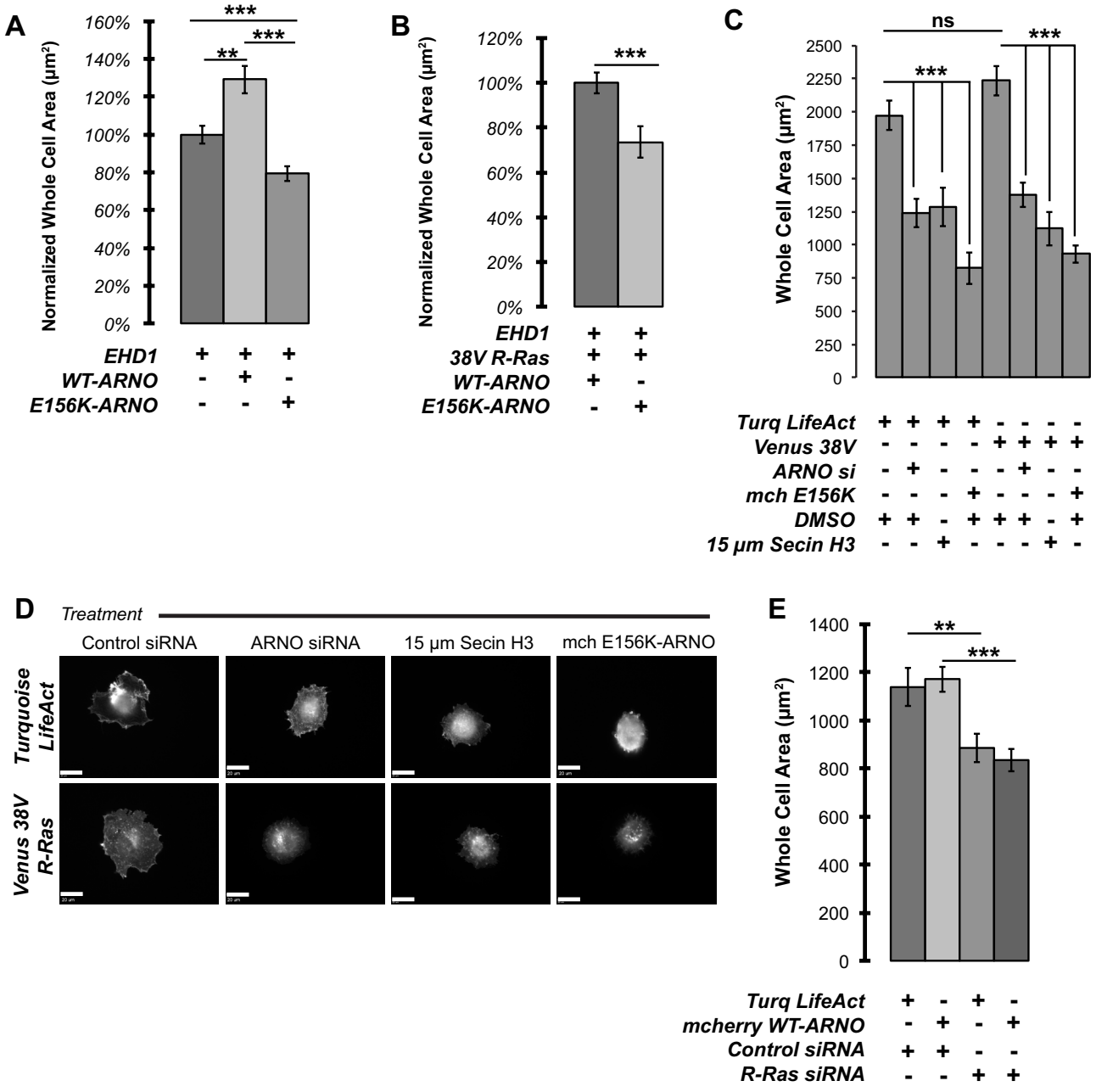

FIGURE 5: Internal accumulation of R-Ras caused by GEF-inactive cytohesin-2/ARNO correlates with inhibited cell spreading. Whole-cell area was measured in cells from Figure 1 (A) and Figure 3 (B). (C) Cells were transfected with universal negative control siRNA (Invitrogen) or siRNA targeting human ARNO. The next day, cells were transfected with Lipofectamine 3000 containing the constructs shown. After 48 h, cells were nonenzymatically harvested and seeded onto fibronectin-coated coverslips. Cells were fixed after 35 min of spreading. Whole-cell area was measured using SlideBook 6.0. (D) Representative images of cells close to the average area. The LifeAct channel is shown for control cells, and the R-Ras channel is shown for 38V R-Ras–expressing cells. Samples were analyzed from one experiment using cell numbers 99 for LifeAct control, 96 for 38V R-Ras, 94 for SecinH3 treated, and 74 for E156K expressing. (E) Cells were nonenzymatically harvested and allowed to spread for 20 min on fibronectin-coated coverslips. (LifeAct Cont, 94 cells; LifeAct R-Ras si, 103 cells; ARNO Cont, 88 cells; and ARNO R-Ras si, 119 cells). Measurement from one experiment for statistical significance was done in MiniTab17 using a two-sample *t* test. ***$p < 0.001$, **$p < 0.01$, ns, not significant.

Cytohesin-2/ARNO overexpression could result in rapid turnover of focal adhesions, thus decreasing the overall number. Most of the larger adhesions in WT-ARNO cells were found closer to the peripheral plasma membrane, in contrast to LifeAct controls, which had focal adhesions throughout the whole area of the cell. These data support a model in which cytohesin-2/ARNO is required to properly localize R-Ras to establish R-Ras–dependent effects on spreading and focal adhesion formation.

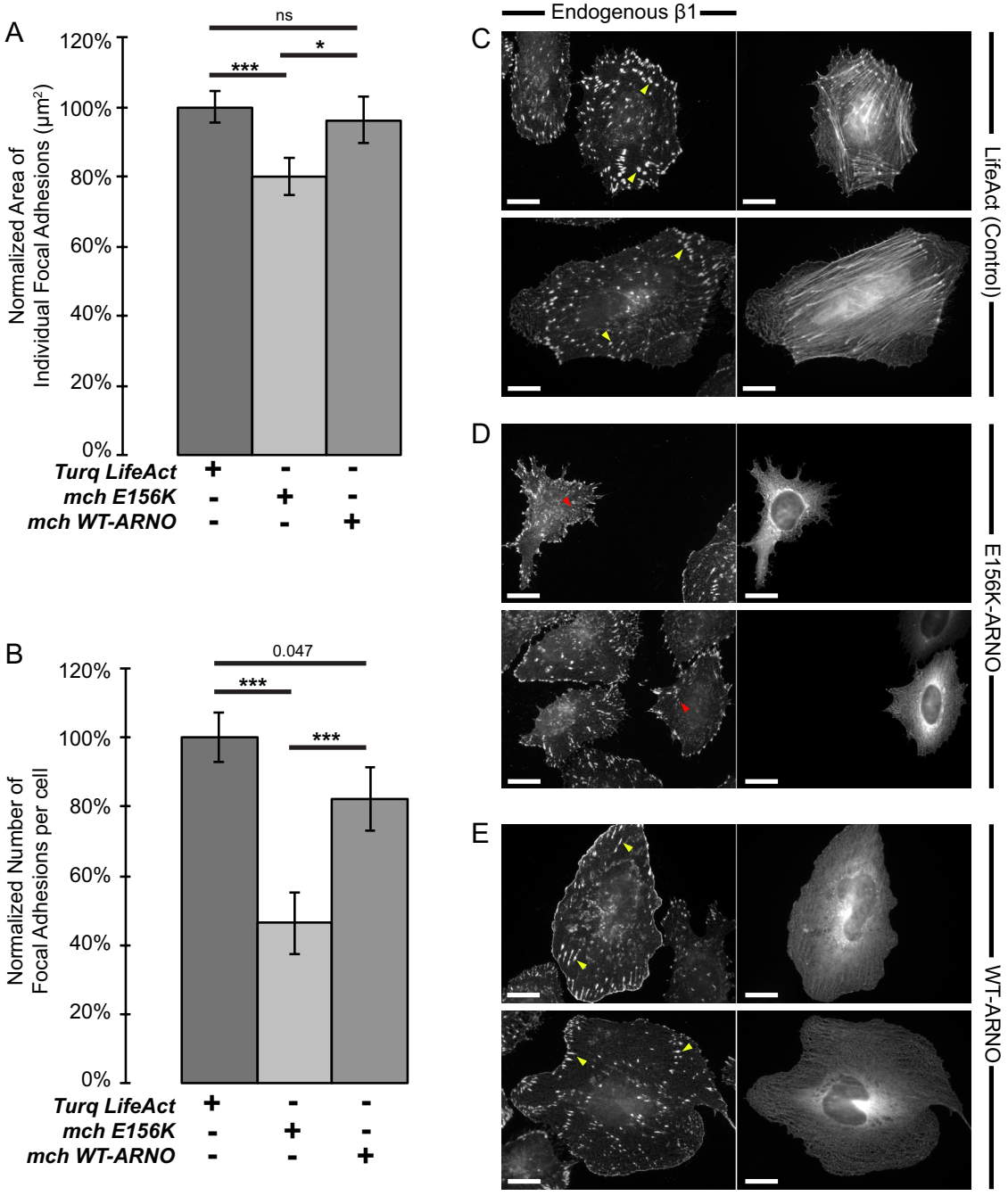

FIGURE 6: Expression of E156K-ARNO causes a reduction in focal adhesion size and number. Cells were transfected with Turquoise LifeAct, mCherry WT-ARNO, or mCherry E156K-ARNO and subsequently stained for endogenous β1-integrin (Alexa 488 secondary antibody was used for ARNO-transfected cells; Alexa 594 was used for LifeAct controls). (A, B) β1-Integrin channels were masked to highlight focal adhesions, and the area (A) and number (B) of those objects was exported using SlideBook 6.0 (LifeAct, 31 cells; mchE156K-ARNO, 33 cells; mchWT-ARNO, 24 cells). (C–E) Representative images showing focal adhesion distribution. Left, immunostained endogenous β1-integrin. Right, LifeAct control (C), E156K-ARNO (D), or WT-ARNO (E). Yellow arrows show large adhesions; red arrows show small adhesions. Measurement from one experiment for statistical significance was done in MiniTab17 using a two-sample *t* test. ***$p < 0.001$, *$p < 0.05$; ns, not significant.

Disruption of R-Ras/ARNO signaling blocks serum-stimulated α5-integrin recycling and peripheral plasma membrane localization of R-Ras

We previously showed that cytohesin-2/ARNO is required for stimulated β1-integrin recycling, cell spreading, and migration (Oh and Santy, 2010, 2012). Given that R-Ras functions in promoting recycling and proper distribution of integrin, namely β1 (Conklin *et al.*, 2010), and EHD1 is required for β1-integrin recycling, spreading, and migration (Jović *et al.*, 2007), we wondered whether blockage of the R-Ras/ARNO signaling module could inhibit integrin and

R-Ras recycling to the plasma membrane. R-Ras/ARNO signaling was inhibited three different ways in cells expressing a Venus-tagged α5-integrin: by expressing 43N R-Ras or E156K-ARNO or treating cells with the cytohesin inhibitor SecinH3. Because we used an antibody that recognizes active β1, we could confirm that R-Ras and active β1 are both found at the plasma membrane after serum stimulation. Cells expressing Turquoise WT R-Ras showed high intracellular R-Ras, which highly localized with α5-integrin before serum stimulation (Figure 7A; 0 min). After 5 min of serum stimulation, WT R-Ras was seen at the plasma membrane with Venus α5-integrin (Figure 7A, 5 min). At 15 min, some cells displayed plasma membrane– localized R-Ras and α5-integrin all around the cell periphery (Figure 7A, 15 min). When WT R-Ras was substituted with 43N R-Ras, cells no longer responded to serum. Punctate 43N R-Ras colocalized with α5β1-integrin puncta at 0, 5, and 15 min (Figure 7B). Remarkably, stimulated recycling of integrin and R-Ras was also inhibited in cells treated simultaneously with serum and cytohesin inhibitor SecinH3 (Figure 7C). Although SecinH3 inhibits all cytohesins, we have shown that cytohesin-3/GRP1 has opposing effects on spreading and migration and that GRP1 is nonessential for β1-integrin recycling (Oh and Santy, 2010). Expression of E156K-ARNO phenocopies SecinH3 treatment and blocks stimulated recruitment of R-Ras (Figure 7D). Surprisingly, very few cells contained significant amounts of R-Ras in tubules. We believe that the permeabilization required for antibody staining dissolves EHD1 tubes in most cells. In summary, R-Ras/ARNO signaling is specialized for stimulated recycling of α5-integrin, whether by serum induction or spreading on fibronectin matrix.

To establish EHD1-positive endosomes as a compartment for α5-integrin and cytohesin-2/ARNO as a regulator of the α5-integrin recycling, we used siRNA targeting endogenous cytohesin-2/ARNO and asked whether we could rescue serum-stimulated recycling of α5-integrin by expressing mCherry WT-ARNO. At time 0, both WT-ARNO– and E156K-ARNO–expressing cells showed high perinuclear distribution of EHD1 and α5-integrin (Figure 8, A and B). After 1 and 5 min of serum treatment, α5-integrin and EHD1 reorganized away from the perinucleus and diffused toward the cell periphery in cells expressing WT-ARNO (Figure 8A). However, in cells expressing E156K-ARNO, α5-integrin and EHD1 remained highly intracellular and perinuclear (Figure 8B). Taken together, these data demonstrate that R-Ras and α5β1-integrin recycle through an EHD1-positive compartment under control of cytohesin-2/ARNO.

DISCUSSION

A clear model of how R-Ras promotes cell spreading and adhesion has remained elusive due to our limited understanding of how R-Ras traffics. Here we established EHD1-positive endosomes as a novel compartment for cytohesin-2/ARNO and R-Ras. We showed that cytohesin-2/ARNO is required for R-Ras recycling through the ERC and for effects of R-Ras on cell spreading and focal adhesion formation. Spreading defects caused by R-Ras knockdown cannot be rescued by cytohesin-2/ARNO overexpression. Finally, cytohesin-2/ARNO is required for serum-stimulated peripheral plasma membrane localization of R-Ras and α5-integrin.

The use of a GEF-inactive mutant of cytohesin-2/ARNO gave us a unique ability to establish a connection between cytohesin-2/ARNO, EHD1, and R-Ras. Expression of a GDP-locked mutant of ARF6 has been shown to disrupt formation of the EHD1 compartment itself (Caplan *et al.*, 2002) and thus would likely not phenocopy the effects of E156K-ARNO on EHD1 endosomes. We believe there are several possible mechanisms to explain how E156K-ARNO

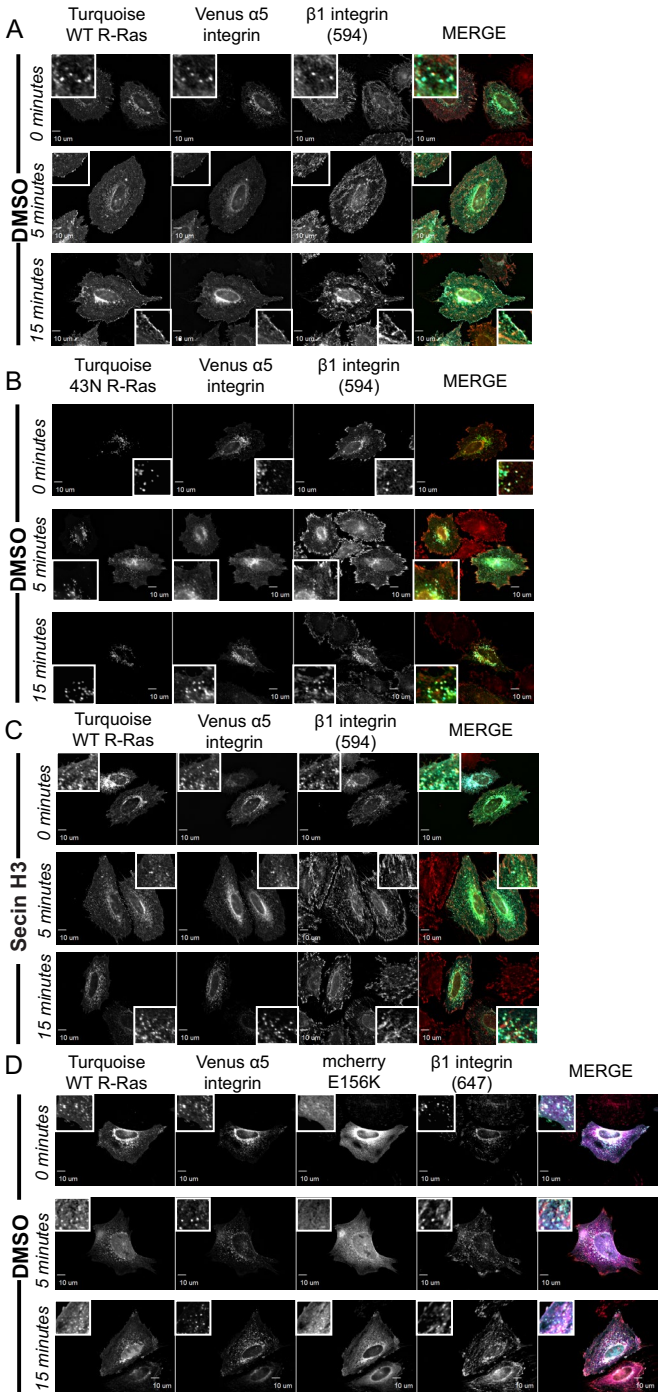

FIGURE 7: Blockage of the R-Ras/ARNO signaling module inhibits serum-stimulated recycling of R-Ras and α5-integrin to the plasma membrane. Transfected HeLa cells plated on fibronectin-coated coverslips were allowed to recover in normal growth medium with serum for 5 h. Serum-free medium was added to recovered cells overnight. The next day, HeLa cells were treated with warm medium containing 0% serum (time 0) or 20% serum for 5 and 15 min. After the indicated time, cells were fixed and stained for endogenous β1-integrin. SecinH3, 15 μM, was added at the same time as 20% serum shock. Equal amounts of DMSO were added to all other samples. In the merged images, R-Ras is pseudocolored cyan, α5-integrin is green, 594 and 647 β1-integrin are red, and E156K-ARNO is magenta. WT R-Ras control, 111 cells; 43N R-Ras, 42 cells; Secin-treated cell, 67 cells; E156K expressing, 108 cells. Scale bars, 10 μm.

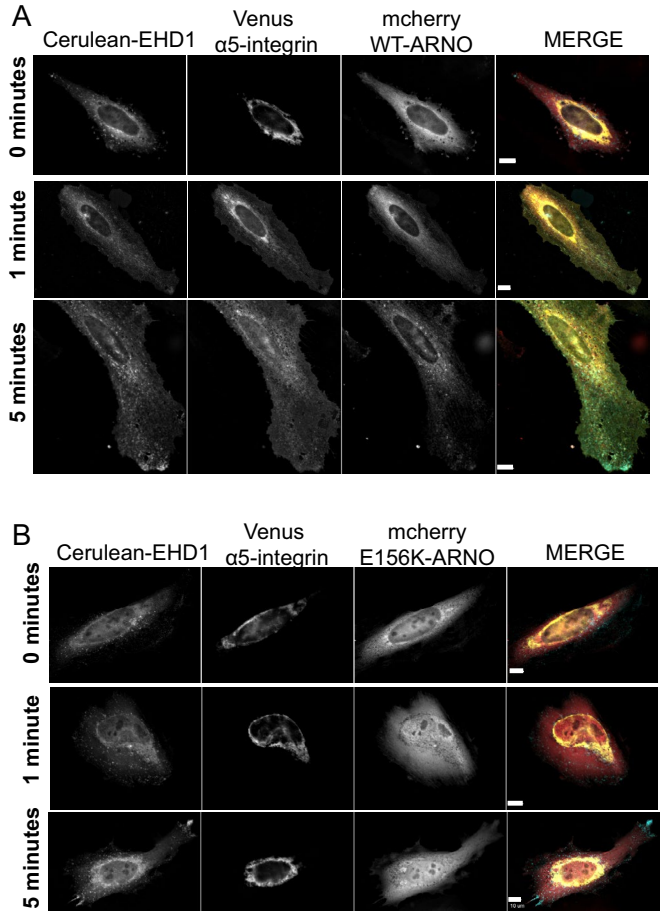

FIGURE 8: GEF-inactive E156K-ARNO inhibits α5-integrin recycling upon serum stimulation. HeLa cells were subjected to Neon electroporation to knock down endogenous cytohesin-2/ARNO and seeded onto fibronectin-coated coverslips. After 16 h of knockdown, cells were transiently transfected with constructs expressing Cerulean-EHD1, Venus-α5-integrin, and siRNA-resistant mCherry WT-ARNO (A) or GEF-inactive mCherry siRNA-resistant E156K-ARNO (B) and were allowed to express the proteins for 24 h. The next day, cells were treated with 20% FBS for 0, 1, or 5 min to stimulate integrin recycling and viewed under a wide-field microscope. In the merged images, EHD1 is pseudocolored cyan, α5-integrin is yellow, and ARNO is red. WT-ARNO cells analyzed, 67; E156K cells analyzed, 133. Scale bars, 10 μm.

inhibits R-Ras recycling and causes a build-up of R-Ras/EHD1 internally. Our images of permeabilized cells (Figure 1) suggest that there is recruitment of WT- and E156K-ARNO onto endosomal membranes containing EHD1. Thus E156K-ARNO would be in a position to associate with ARF-GDP but fails to perform the exchange reaction, thus preventing exocytosis from EHD1-positive endosomes and recycling back out to the plasma membrane (Béraud-Dufour *et al.*, 1998; Renault *et al.*, 2003). In addition, cytohesins function through a positive feedback loop by which autoinhibition is relieved by associating with ARF-GTP through their PH domains (DiNitto *et al.*, 2007; Stalder *et al.*, 2011). Expression of E156K-ARNO could in turn reduce the levels of cytohesin-2/ARNO that are relieved of autoinhibition and thus recruited onto membrane. Depletion of peripheral ARF1-GTP and ARF6-GTP by E156K-ARNO likely inhibits recycling of R-Ras, as well as cell spreading. Cytohesin-2/ARNO is a more efficient GEF for ARF1, and ARF6 binds more strongly to the PH domain of cytohesin-2/ARNO to allow for membrane recruitment (Cohen *et al.*, 2007). Indeed, expression of dominant-negative ARF1 prevents full spreading rescue when R-Ras effector RLIP76 is knocked down (Goldfinger, 2006). RLIP76 has been shown to associate directly with cytohesin-2/ARNO (Lee *et al.*, 2014) and could aid in directly recruiting cytohesin-2/ARNO onto membrane tubules. No one has investigated whether RLIP76 traffics through the ERC.

Knockdown of R-Ras or expression of dominant-negative R-Ras has been shown by several groups to inhibit cell spreading, migration, and adhesion (Wozniak *et al.*, 2005; Goldfinger, 2006; Sandri *et al.*, 2012; Wurtzel *et al.*, 2012). Our data show that spreading deficiencies caused by R-Ras knockdown cannot be rescued by cytohesin-2/ARNO while cells are actively spreading. We also demonstrate that R-Ras must be activated to associate with EHD1-positive endosomes at the ERC. Thus our model provides two key steps required for R-Ras-dependent spreading and adhesion formation (Figure 9): 1) R-Ras must be activated to reach EHD1-positive endosomes (Figure 9, #1) and 2) the GEF-activity of cytohesin-2/ARNO is required for R-Ras/integrin recycling (Figure 9, #2). It is conceivable that R-Ras activation may be required to reach any endosomal compartment, as dominant-negative R-Ras has only been shown to localize with dominant-negative ARF6 puncta (Furuhjelm and Peränen, 2003) and, to our knowledge, no other Rab markers. This could explain why 43N R-Ras wobbles back and forth in no particular direction in live cells (Wurtzel *et al.*, 2012) and its localization is not affected by cytohesin-2/ARNO knockdown.

This and previous studies (Oh and Santy, 2010, 2012) establish a role for cytohesin-2/ARNO in the recycling of integrins. EHD1 is required for β1-integrin recycling and turnover of focal adhesions (Jović *et al.*, 2007). Of interest, migration of mouse embryonic fibroblasts isolated from EHD1-knockout mice is inhibited on fibronectin matrix. However, on vitronectin, which is recognized by β3-integrin (Hynes, 2002), EHD1 levels do not change the migration efficiency (Jović *et al.*, 2007). Immunofluorescence experiments performed in this study used cells plated on fibronectin, which is recognized by α5β1-integrin receptors. GEF-inactive cytohesin-2/ARNO causes a perinuclear accumulation of α5-integrin in serum-stimulated cells. Thus we support a model in which EHD1/ARNO controls recycling of integrin heterodimers containing β1. BRAG2, also a GEF for ARF6, has been shown to regulate β1-integrin endocytosis in HeLa cells (Dunphy *et al.*, 2006). Cytohesin-2/ARNO and BRAG2 may work in concert by regulating integrin recycling and internalization, respectively (Dunphy *et al.*, 2006).

The mechanism by which cytohesin-2/ARNO dually controls integrin and R-Ras recycling is not clear. In our model, cytohesin-2/ARNO recycles R-Ras to areas where it is needed. However, a possible function of R-Ras might be to chaperone integrin to the ERC, such that cytohesin-2/ARNO can recycle both components concurrently. We showed in serum-stimulated cells that dominant-negative R-Ras localizes with high levels of α5-integrin in immunostained cells (Figure 7). The reduction in focal adhesion size caused by E156K-ARNO (Figure 6) is most likely due to inhibition of R-Ras and β1-integrin recycling. A similar phenotype has been demonstrated when expressing 43N R-Ras in HeLa cells (Furuhjelm and Peränen, 2003). In different cell types, others have proposed that R-Ras does not regulate the recycling of total integrin to the plasma membrane (Conklin *et al.*, 2010; Sandri *et al.*, 2012) but instead the endocytosis of activated integrin (Sandri *et al.*, 2012). Therefore cytohesin-2/ARNO–induced ARF-activation could be required to recycle R-Ras to integrin-enriched sites near the plasma membrane.

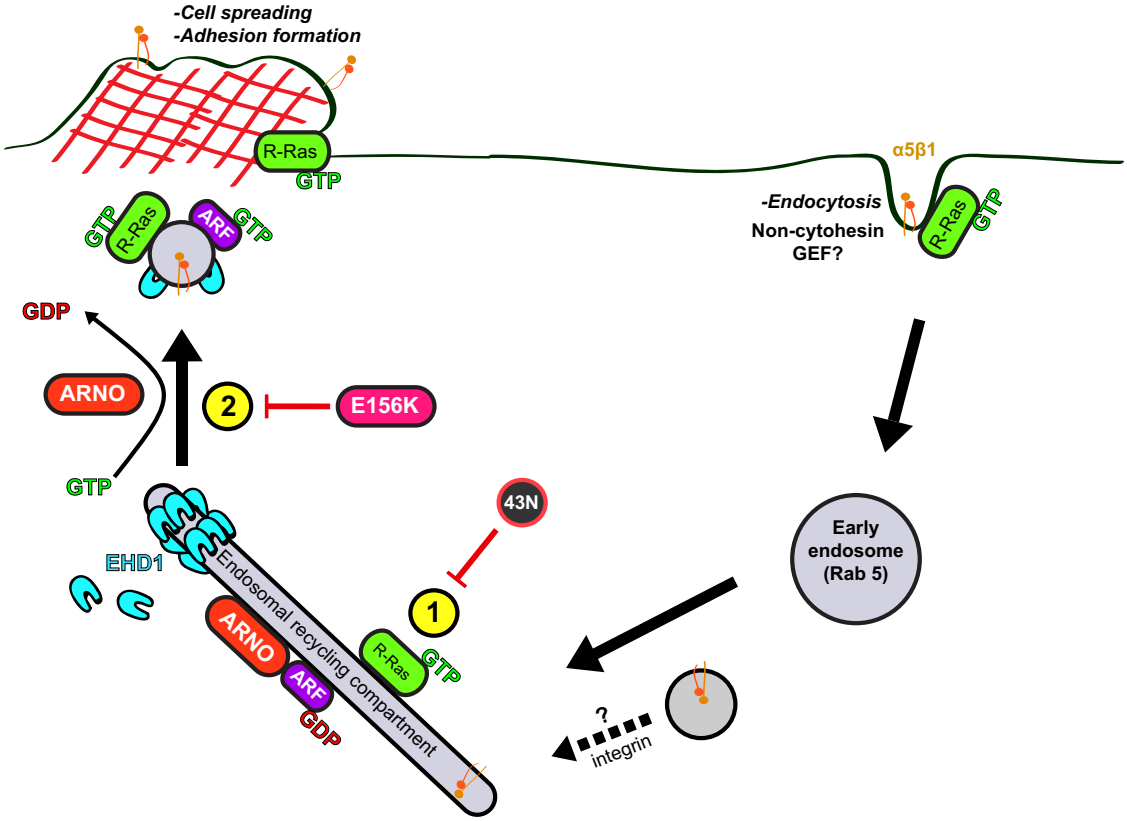

FIGURE 9: Model of cytohesin-2/ARNO–dependent recycling of R-Ras. R-Ras/integrins are internalized, perhaps through a noncytohesin ARF-GEF (i.e., BRAG2), and traffic to Rab5 early endosomes. Active R-Ras is recruited onto an EHD1-positive ERC compartment that contains integrin and cytohesin-2/ARNO (1). Cytohesin-2/ARNO-induced ARF-activation is required for exocytosis of R-Ras from the ERC (2). Peripherally localized R-Ras is able to enhance cell spreading and establish adhesions.

Future experiments are needed to determine the role of R-Ras/ARNO in the activation of Rac1 in epithelial cells. Both Rac1 and Rho play important roles in establishing focal complexes and focal adhesions (Nobes and Hall, 1995; Rottner *et al.*, 1999). We showed that cytohesin-2/ARNO associates with the scaffolding protein GRASP, which directly recruits DOCK180 (Attar and Santy, 2013). This interaction is required for cytohesin-2/ARNO–induced Rac1 activation and migration (Santy *et al.*, 2005; White *et al.*, 2010). If the coiled-coil domain is deleted, cytohesin-2/ARNO can still activate ARF6, but Rac1 is not activated, and thus migration is inhibited (White *et al.*, 2010). Therefore, even if R-Ras is efficiently recycled through ARF6-GTP, Rac1 activation would still be required to establish cell–extracellular matrix adhesions.

R-Ras may directly or indirectly stimulate the GEF activity of cytohesin-2/ARNO. RLIP76 binds R-Ras-GTP (Goldfinger, 2006) and interacts with cytohesin-2/ARNO to stimulate ARF6 and Rac1 activation (Lee *et al.*, 2014). In fibroblasts, cytohesin-2/ARNO overexpression has been shown to rescue cell spreading in cells in which endogenous RLIP76 is reduced (Goldfinger, 2006). Similarly, RLIP76 overexpression can rescue cell spreading and ARF6 activation in cells expressing dominant-negative R-Ras. Thus cytohesin-2/ARNO functions downstream of R-Ras/RLIP76. R-Ras, and cytohesin-2/ARNO may not perform in a direct linear pathway in HeLa cells. Intriguingly, R-Ras localizes to focal adhesions in HeLa cells (Furuhjelm and Peränen, 2003) but not fibroblasts (Wurtzel *et al.*, 2012). In support of this model, MDCK epithelial cells overexpressing cytohesin-2/ARNO fail to activate Rac1 and migrate when GRASP or CNK3/IPCEF1 levels are reduced (White *et al.*, 2010). It is tempting to speculate that the other cytohesin-2/ARNO–binding proteins, such as CNK3/IPCEF1, could interact with RLIP76 to regulate migration in epithelial cells. Future studies will need to determine how these factors come together to form a signaling module.

MATERIALS AND METHODS

Antibodies and reagents

TS2/16 anti–β1 integrin antibody was purchased from Santa Cruz Biotechnology (Santa Cruz, CA). Alexa Fluor–conjugated anti-mouse secondary antibodies (488, 594, 647) were from Jackson ImmunoResearch Laboratories (West Grove, PA). SecinH3 was purchased from EMD Millipore (Billerica, MA). Human fibronectin matrix was obtained from Corning (Corning, NY).

Plasmid constructs

Myc-tagged human R-Ras WT and mutant (38V and 43N) were a gift from L. E. Goldfinger (Temple University School of Medicine, Philadelphia, PA). Primers were designed to clone myc-R-Ras into pCXN2 mammalian expression vector containing the gene for mCherry, Venus, or Turquoise fluorescent tags. R-Ras constructs were cloned using the primers NotRRasRev (5-CTGGATGCGGCCGCTCATCACTACAGGAGGACGCAGGGGCA-3′) and either KpnMycRRasWT (5-GGTACCGCCACCATGGAACAAAAACTAATATCGGAAGAAGATCTA-3′) for WT R-Ras or KpnMycFwd (5-CACGGGGTACCGCCACCATGGAGCAGAAGCTGATCTCC-3′) for mutant R-Ras. Cerulean-EHD1, Venus Rab8a, and Venus Rab11a constructs were a gift

from Jim Goldenring (Vanderbilt University, Nashville, TN). Human GFP α5-integrin (plasmid 15238; deposited by Rick Horwitz from the University of Virginia, Charlottesville, VA; Laukaitis *et al.*, 2001) and Turquoise LifeAct (plasmid 36201; deposited by Dorus Gadella from the University of Virginia; Goedhart *et al.*, 2012) were purchased from AddGene (Cambridge, MA). α5-integrin was excised from its original vector using *Kpn*I and ligated into pCDNA3 with a C-terminal Venus tag. Control and siRNA-resistant versions of mCherry WT-ARNO and mCherry E156K-ARNO have been previously described (Oh and Santy, 2012).

Cell lines

HeLa cells were maintained in DMEM supplemented with 10% fetal bovine serum, 1% penicillin, streptomycin, and Fungizone, and 2 mM L-glutamine. HeLa cells were cultured at 37°C and 5% CO_2.

siRNA-mediated knockdown

siRNA duplexes targeting the sequence 5-GCAAUGGGCAGGAAGAAGU-3 targeting human cytohesin 2/ARNO were purchased from Dharmacon (Lafayette, CO), and negative universal control siRNA (46-2002) was purchased from Invitrogen (Carlsbad, CA). Human R-Ras siRNA pool was purchased from Dharmacon (M-010352-02). The siRNAs (200 nM) were transfected into 1×10^6 HeLa cells by using a Neon Transfection System (Invitrogen) according to the manufacturer's recommended protocol (1005 V, 35 ms, 2x). Altogether, 1×10^5 cells were plated on square coverslips coated with fibronectin.

Immunofluorescence and image analysis

All HeLa cells were plated on flame-sterilized, fibronectin-coated (EMD Millipore) coverslips (20 µg/ml) and mounted using Prolong Gold Antifade reagent (Life Technologies). Microscopic images were taken using an Olympus IX83 inverted microscope (Tokyo, Japan) equipped with SlideBook 6.0 software (Intelligent Imaging Innovations, Denver, CO) for image analysis. To assess EHD1 tube formation in SlideBook 6.0, raw images were treated with a 2D Laplacian filter to resolve endosomes. EHD1 channels were masked to include intracellular EHD1 endosomes. Nonendosomal areas (i.e., cell debris and spiked protrusions) were erased from masks on all images. For ARNO-knockdown experiments, masks were gated to exclude objects <0.5 μm^2 (43N R-Ras masks were exported with 0.1-μm^2 gating), and the internal masked endosomal area (square micrometers) was exported. Whole-cell area (square micrometers) was generated by masking an unfiltered channel. To assess the amount of internal EHD1, the filtered EHD1 endosomal area was divided by the whole-cell area. For morphometry analysis, the same masks were exported as individual objects. Objects of a given size range were counted and calculated as percentage of total objects. Raw values from these masks were loaded into MiniTab 17 software. Two-sample *t* tests were carried out in MiniTab 17. All means shown are ± SE.

Reverse transcription PCR

Total RNA was extracted from HeLa cells using the RNeasy Plus kit (Qiagen, Valencia, CA). Custom cytohesin-2/ARNO primers were used to amplify 183-291 of cytohesin-2/ARNO (humanARNOfwd, 5-ACACGTGCTATGTGCTGTCC-3; humanARNOrev, 5-TAGTAGAGGCAGTTGTCTGTGAGG-3); 53–169 of human GRP1 (humanGRP1fwd, 5-CGACAATCTAACTTCCGTAGAGG; humanGRP1rev, 5-TCATGCGATCAATCTTCTGC), and 46–147 of human R-Ras (RRasFwd, 5-CCATCCAGTTCATCCAGTCC-3; RRasRev, 5-CTCCAGATCTGCCTTGTTCC-3). ReadyMade primers to amplify glyceraldehyde-3-phosphate dehydrogenase (GAPDH) were obtained from Integrated DNA Technologies (Coralville, IA). Reverse transcription (RT)-PCR was performed with 100 ng of total RNA as template for GAPDH and 0.5 µg as template for ARNO and GRP1 using the Qiagen One-Step RT-PCR kit. RT-PCR reactions were treated with RNase cocktail (Ambion, Austin, TX) for 30 min at 37 degrees before gel electrophoresis. Band intensities were measured in ImageJ software (National Institutes of Health, Bethesda, MD).

Serum stimulation

HeLa cells were Neon transfected, as described. Cells were allowed to recover for 5 h in antibiotic-free medium with 10% serum. After 5 h, cells were washed with phosphate-buffered saline (PBS), and serum-free/antibiotic-free medium containing L-glutamine was added for overnight serum starvation. After 18 h, cells were treated with dimethyl sulfoxide (DMSO; 1:1000) and 20% fetal bovine serum (FBS) in warm DMEM for 5 or 15 min. Time 0 cells were only treated with DMSO (1:1000) in warm DMEM. SecinH3 (1:1000 or 15 µM) was added to warm DMEM containing 0 or 20% serum before stimulation. After stimulation, cells were washed with PBS and fixed with 4% paraformaldehyde. For staining, cells were blocked and permeabilized using 0.1% Triton X-100 and 5% normal goat serum for 30 min. TS2/16 anti–β1 integrin antibody (Santa Cruz Biotechnology) was diluted in 1% bovine serum albumin (BSA) and 0.1% Triton X-100 in PBS, and coverslips were allowed to incubate for 1 h. Cells were washed in PBS, and mouse Alexa 594 or Alexa 647 (Jackson ImmunoResearch Laboratories) antibody was diluted and incubated for 1 h. Cells were washed in PBS and distilled water and mounted using ProLong Gold Antifade reagent (Life Technologies).

Transfection of siRNA-treated cells

Cells treated with siRNA (as described earlier) were transfected for siRNA using the Neon Transfection System. After 24 h, cells were transfected with Lipofectamine 3000 (Invitrogen) according to the manufacturer's instructions and allowed to express overnight to achieve 48 h of knockdown. After 48 h, the cells were fixed and mounted as described.

Saponin permeabilization

Cells were transfected as described and allowed to express with serum overnight. The next day, cells were washed twice with PBS, and permeabilization buffer (modified from Richardson *et al.*, 2004 ; 80 mM 1,4-piperazinediethanesulfonic acid, pH 6.5, 5 mM ethylene glycol tetraacetic acid, 1 mM $MgCl_2$, 0.02% saponin, and sterile water) was added for 1 min. Cells were washed quickly with PBS and fixed and mounted as described.

Cell spreading assay

We transfected 1×10^6 cells with universal control siRNA or siRNA targeting human ARNO, using Neon. Cells to be treated with vector constructs were added to 12-well plates (6×10^4), and cells to be harvested for RNA were plated on 6-cm plates (3.5×10^5). The next day, cells were transfected with Turquoise LifeAct, Venus 38V R-Ras, or mCherry-ARNO and re-treated with siRNA (control siRNA, hARNO siRNA, or hR-Ras siRNA) using Lipofectamine 3000 according to the manufacturer's recommended instructions. Cells on 6-cm plates were harvested for total RNA using the RNeasy Plus Kit (Qiagen). Cells on 12-well plates were nonenzymatically harvested using 4 mM EGTA and 1 mM EDTA for 30 min. Cells were plated at subconfluency (30–40%) onto fibronectin-coated coverslips and allowed to spread for 20 or 35 min in FlouroBrite media

(Life Technologies) containing 0.2% BSA, 10% FBS, and 2 mM L-glutamine. Cells were fixed and mounted onto coverglasses using ProLong Gold Antifade reagent (Life Technologies).

ACKNOWLEDGMENTS

We thank Larry Goldfinger (Temple University) for kindly providing the R-Ras constructs and Jim Goldenring (Vanderbilt University) for the EHD1 and Rab constructs. This work was supported by grants from the American Cancer Society (RSG-09-168-01-CSM) and the National Institutes of Health (R01 DK093729) to L.C.S.

REFERENCES

Attar MA, Salem JC, Pursel HS, Santy LC (2012). CNK3 and IPCEF1 produce a single protein that is required for HGF dependent Arf6 activation and migration. Exp Cell Res 318, 228–237.

Attar MA, Santy LC (2013). The scaffolding protein GRASP/Tamalin directly binds to Dock180 as well as to cytohesins facilitating GTPase crosstalk in epithelial cell migration. BMC Cell Biol 14, 9.

Beemiller P, Hoppe AD, Swanson JA (2006). A phosphatidylinositol-3-kinase-dependent signal transition regulates ARF1 and ARF6 during Fcgamma receptor-mediated phagocytosis. PLoS Biol 4, e162.

Béraud-Dufour S, Robineau S, Chardin P, Paris S, Chabre M, Cherfils J, Antonny B (1998). A glutamic finger in the guanine nucleotide exchange factor ARNO displaces Mg2+ and the beta-phosphate to destabilize GDP on ARF1. EMBO J 17, 3651–3659.

Birchmeier C, Birchmeier W, Gherardi E, Vande Woude GF (2003). Met, metastasis, motility and more. Nat Rev Mol Cell Biol 4, 915–925.

Bryant DM, Mostov KE (2008). From cells to organs: building polarized tissue. Nat Rev Mol Cell Biol 9, 887–901.

Cai B, Giridharan SSP, Zhang J, Saxena S, Bahl K, Schmidt JA, Sorgen PL, Guo W, Naslavsky N, Caplan S (2013). Differential roles of C-terminal Eps15 homology domain proteins as vesiculators and tubulators of recycling endosomes. J Biol Chem 288, 30172–30180.

Caplan S, Naslavsky N, Hartnell LM, Lodge R, Polishchuk RS, Donaldson JG, Bonifacino JS (2002). A tubular EHD1-containing compartment involved in the recycling of major histocompatibility complex class I molecules to the plasma membrane. EMBO J 21, 2557–2567.

Casanova JE (2007). Regulation of Arf activation: the Sec7 family of guanine nucleotide exchange factors. Traffic 8, 1476–1485.

Caswell PT, Spence HJ, Parsons M, White DP, Clark K, Cheng KW, Mills GB, Humphries MJ, Messent AJ, Anderson KI, *et al.* (2007). Rab25 associates with alpha5beta1 integrin to promote invasive migration in 3D microenvironments. Dev Cell 13, 496–510.

Cohen LA, Honda A, Varnai P, Brown FD, Balla T, Donaldson JG (2007). Active Arf6 recruits ARNO/cytohesin GEFs to the PM by binding their PH domains. Mol Biol Cell 18, 2244–2253.

Conklin MW, Ada-Nguema A, Parsons M, Riching KM, Keely PJ (2010). R-Ras regulates beta1-integrin trafficking via effects on membrane ruffling and endocytosis. BMC Cell Biol 11, 14.

Davies JCB, Tamaddon-Jahromi S, Jannoo R, Kanamarlapudi V (2014). Cytohesin 2/ARF6 regulates preadipocyte migration through the activation of ERK1/2. Biochem Pharmacol 92, 651–660.

DiNitto J, Delprato A, Lee M, Cronin T, Huang S, Guilherme A, Czech MP, Lambright DG (2007). Structural basis and mechanism of autoregulation in 3-phosphoinositide-dependent Grp1 family Arf GTPase exchange factors. Mol Cell 28, 569–583.

Donaldson JG, Jackson CL (2011). ARF family G proteins and their regulators: roles in membrane transport, development and disease. Nat Rev Mol Cell Biol 12, 362–375.

Donaldson JG, Porat-Shliom N, Cohen LA (2009). Clathrin-independent endocytosis: a unique platform for cell signaling and PM remodeling. Cell Signal 21, 1–6.

D'Souza-Schorey C, Chavrier P (2006). ARF proteins: roles in membrane traffic and beyond. Nat Rev Mol Cell Biol 7, 347–358.

Dunphy JL, Moravec R, Ly K, Lasell TK, Melancon P, Casanova JE (2006). The Arf6 GEF GEP100/BRAG2 regulates cell adhesion by controlling endocytosis of beta1 integrins. Curr Biol 16, 315–320.

Farooqui R, Fenteany G (2005). Multiple rows of cells behind an epithelial wound edge extend cryptic lamellipodia to collectively drive cell-sheet movement. J Cell Sci 118, 51–63.

Fenteany G, Janmey PA, Stossel TP (2000). Signaling pathways and cell mechanics involved in wound closure by epithelial cell sheets. Curr Biol 10, 831–838.

Frank SR, Hatfield JC, Casanova JE (1998). Remodeling of the actin cytoskeleton is coordinately regulated by protein kinase C and the ADP-ribosylation factor nucleotide exchange factor ARNO. Mol Biol Cell 9, 3133–3146.

Furuhjelm J, Peränen J (2003). The C-terminal end of R-Ras contains a focal adhesion targeting signal. J Cell Sci 116, 3729–3738.

Gao Q, Liu W, Cai J, Li M, Gao Y, Lin W, Li Z (2014). EphB2 promotes cervical cancer progression by inducing epithelial-mesenchymal transition. Hum Pathol 45, 372–381.

Goedhart J, von Stetten D, Noirclerc-Savoye M, Lelimousin M, Joosen L, Hink MA, van Weeren L, Gadella TWJ, Royant A (2012). Structure-guided evolution of cyan fluorescent proteins towards a quantum yield of 93%. Nat Commun 3, 751.

Goldfinger LE (2006). RLIP76 (RalBP1) is an R-Ras effector that mediates adhesion-dependent Rac activation and cell migration. J Cell Biol 174, 877–888.

Hafner M, Schmitz A, Grüne I, Srivatsan SG, Paul B, Kolanus W, Quast T, Kremmer E, Bauer I, Famulok M (2006). Inhibition of cytohesins by SecinH3 leads to hepatic insulin resistance. Nature 444, 941–944.

Hattula K, Furuhjelm J, Tikkanen J, Tanhuanpää K, Laakkonen P, Peränen J (2006). Characterization of the Rab8-specific membrane traffic route linked to protrusion formation. J Cell Sci 119, 4866–4877.

Hiester KG, Santy LC (2013). The cytohesin coiled-coil domain interacts with threonine 276 to control membrane association. PLoS One 8, e82084.

Holly SP, Larson MK, Parise LV (2005). The unique N-terminus of R-ras is required for Rac activation and precise regulation of cell migration. Mol Biol Cell 16, 2458–2469.

Hughes PE, Oertli B, Hansen M, Chou FL, Willumsen BM, Ginsberg MH (2002). Suppression of integrin activation by activated Ras or Raf does not correlate with bulk activation of ERK MAP kinase. Mol Biol Cell 13, 2256–2265.

Hughes PE, Renshaw MW, Pfaff M, Forsyth J, Keivens VM, Schwartz MA, Ginsberg MH (1997). Suppression of integrin activation: a novel function of a Ras/Raf-initiated MAP kinase pathway. Cell 88, 521–530.

Hynes RO (2002). Integrins: bidirectional, allosteric signaling machines. Cell 110, 673–687.

Jeong H-W, Nam J-O, Kim I-S ((2005). The COOH-terminal end of R-Ras alters the motility and morphology of breast epithelial cells through Rho/Rho-kinase. Cancer Res 65, 507–515.

Jović M, Naslavsky N, Rapaport D, Horowitz M, Caplan S (2007). EHD1 regulates beta1 integrin endosomal transport: effects on focal adhesions, cell spreading and migration. J Cell Sci 120, 802–814.

Keely PJ, Rusyn EV, Cox AD, Parise LV (1999). R-Ras signals through specific integrin alpha cytoplasmic domains to promote migration and invasion of breast epithelial cells. J Cell Biol 145, 1077–1088.

Khwaja A, Lehmann K, Marte BM, Downward J (1998). Phosphoinositide 3-kinase induces scattering and tubulogenesis in epithelial cells through a novel pathway. J Biol Chem 273, 18793–18801.

Komatsu M, Ruoslahti E (2005). R-Ras is a global regulator of vascular regeneration that suppresses intimal hyperplasia and tumor angiogenesis. Nat Med 11, 1346–1350.

Kwong L, Wozniak MA, Collins AS, Wilson SD, Keely PJ (2003). R-Ras promotes focal adhesion formation through focal adhesion kinase and p130(Cas) by a novel mechanism that differs from integrins. Mol Cell Biol 23, 933–949.

Laukaitis CM, Webb DJ, Donais K, Horwitz AF (2001). Differential dynamics of alpha 5 integrin, paxillin, and alpha-actinin during formation and disassembly of adhesions in migrating cells. J Cell Biol 153, 1427–1440.

Lee S, Wurtzel JGT, Goldfinger LE (2014). The RLIP76 N-terminus binds ARNO to regulate PI 3-kinase, Arf6 and Rac signaling, cell spreading and migration. Biochem Biophys Res Commun 454, 560–565.

Lowe DG, Goeddel DV (1987). Heterologous expression and characterization of the human R-ras gene product. Mol Cell Biol 7, 2845–2856.

McHugh BJ, Buttery R, Lad Y, Banks S, Haslett C, Sethi T (2010). Integrin activation by Fam38A uses a novel mechanism of R-Ras targeting to the endoplasmic reticulum. J Cell Sci 123, 51–61.

Mossessova E, Gulbis JM, Goldberg J (1998). Structure of the guanine nucleotide exchange factor Sec7 domain of human arno and analysis of the interaction with ARF GTPase. Cell 92, 415–423.

Mott HR, Owen D (2014). Structure and function of RLIP76 (RalBP1): an intersection point between Ras and Rho signalling. Biochem Soc Trans 42, 52–58.

Nakada M, Niska JA, Tran NL, McDonough WS, Berens ME (2005). EphB2/R-Ras signaling regulates glioma cell adhesion, growth, and invasion. Am J Pathol 167, 565–576.

Nishigaki M, Aoyagi K, Danjoh I, Fukaya M, Yanagihara K, Sakamoto H, Yoshida T, Sasaki H (2005). Discovery of aberrant expression of R-RAS by cancer-linked DNA hypomethylation in gastric cancer using microarrays. Cancer Res 65, 2115–2124.
Nobes CD, Hall A (1995). Rho, rac, and cdc42 GTPases regulate the assembly of multimolecular focal complexes associated with actin stress fibers, lamellipodia, and filopodia. Cell 81, 53–62.
Oh SJ, Santy LC (2010). Differential effects of cytohesins 2 and 3 on beta1 integrin recycling. J Biol Chem 285, 14610–14616.
Oh SJ, Santy LC (2012). Phosphoinositide specificity determines which cytohesins regulate β1 integrin recycling. J Cell Sci 125, 3195–3201.
Palacios F, D'Souza-Schorey C (2003). Modulation of Rac1 and ARF6 activation during epithelial cell scattering. J Biol Chem 278, 17395–17400.
Pellinen T, Arjonen A, Vuoriluoto K, Kallio K, Fransen JAM, Ivaska J (2006). Small GTPase Rab21 regulates cell adhesion and controls endosomal traffic of beta1-integrins. J Cell Biol 173, 767–780.
Powelka AM, Sun J, Li J, Gao M, Shaw LM, Sonnenberg A, Hsu VW (2004). Stimulation-dependent recycling of integrin beta1 regulated by ARF6 and Rab11. Traffic 5, 20–36.
Radhakrishna H, Al-Awar O, Khachikian Z, Donaldson JG (1999). ARF6 requirement for Rac ruffling suggests a role for membrane trafficking in cortical actin rearrangements. J Cell Sci 112(pt 6), 855–866.
Ramos JW, Kojima TK, Hughes PE, Fenczik CA, Ginsberg MH (1998). The death effector domain of PEA-15 is involved in its regulation of integrin activation. J Biol Chem 273, 33897–33900.
Renault L, Guibert B, Cherfils J (2003). Structural snapshots of the mechanism and inhibition of a guanine nucleotide exchange factor. Nature 426, 525–530.
Richardson SCW, Winistorfer SC, Poupon V, Luzio JP, Piper RC (2004). Mammalian late vacuole protein sorting orthologues participate in early endosomal fusion and interact with the cytoskeleton. Mol Biol Cell 15, 1197–1210.
Ridley AJ (2001). Rho GTPases and cell migration. J Cell Sci 114, 2713–2722.
Rincón-Arano H, Rosales R, Mora N, Rodriguez-Castañeda A, Rosales C (2003). R-Ras promotes tumor growth of cervical epithelial cells. Cancer 97, 575–585.
Roberts M, Barry S, Woods A, van der Sluijs P, Norman J (2001). PDGF-regulated rab4-dependent recycling of alphavbeta3 integrin from early endosomes is necessary for cell adhesion and spreading. Curr Biol 11, 1392–1402.
Roland JT, Kenworthy AK, Peranen J, Caplan S, Goldenring JR (2007). Myosin Vb interacts with Rab8a on a tubular network containing EHD1 and EHD3. Mol Biol Cell 18, 2828–2837.
Rottner K, Hall A, Small JV (1999). Interplay between Rac and Rho in the control of substrate contact dynamics. Curr Biol 9, 640–648.
Sabe H (2003). Requirement for Arf6 in cell adhesion, migration, and cancer cell invasion. J Biochem 134, 485–489.
Sandri C, Caccavari F, Valdembri D, Camillo C, Veltel S, Santambrogio M, Lanzetti L, Bussolino F, Ivaska J, Serini G (2012). The R-Ras/RIN2/Rab5 complex controls endothelial cell adhesion and morphogenesis via active integrin endocytosis and Rac signaling. Cell Res 22, 1479–1501.
Santy LC, Casanova JE (2001). Activation of ARF6 by ARNO stimulates epithelial cell migration through downstream activation of both Rac1 and phospholipase D. J Cell Biol 154, 599–610.
Santy LC, Ravichandran KS, Casanova JE (2005). The DOCK180/Elmo complex couples ARNO-mediated Arf6 activation to the downstream activation of Rac1. Curr Biol 15, 1749–1754.
Sethi T, Ginsberg MH, Downward J, Hughes PE (1999). The small GTP-binding protein R-Ras can influence integrin activation by antagonizing a Ras/Raf-initiated integrin suppression pathway. Mol Biol Cell 10, 1799–1809.
Sharma M, Giridharan SS, Rahajeng J, Naslavsky N, Caplan S (2009). MICAL-L1 links EHD1 to tubular recycling endosomes and regulates receptor recycling. Mol Biol Cell 20, 5181–5194.
Song J, Khachikian Z, Radhakrishna H, Donaldson JG (1998). Localization of endogenous ARF6 to sites of cortical actin rearrangement and involvement of ARF6 in cell spreading. J Cell Sci 111(pt 15), 2257–2267.
Stalder D, Barelli H, Gautier R, Macia E, Jackson CL, Antonny B (2011). Kinetic studies of the Arf activator Arno on model membranes in the presence of Arf effectors suggest control by a positive feedback loop. J Biol Chem 286, 3873–3883.
Suzuki J, Kaziro Y, Koide H (2000). Positive regulation of skeletal myogenesis by R-Ras. Oncogene 19, 1138–1146.
Takaya A, Kamio T, Masuda M, Mochizuki N, Sawa H, Sato M, Nagashima K, Mizutani A, Matsuno A, Kiyokawa E, Matsuda M (2007). R-Ras regulates exocytosis by Rgl2/Rlf-mediated activation of RalA on endosomes. Mol Biol Cell 18, 1850–1860.
Tayeb MA, Skalski M, Cha MC, Kean MJ, Scaife M, Coppolino MG (2005). Inhibition of SNARE-mediated membrane traffic impairs cell migration. Exp Cell Res 305, 63–73.
Thiery JP (2002). Epithelial-mesenchymal transitions in tumour progression. Nat Rev Cancer 2, 442–454.
Torii T, Miyamoto Y, Sanbe A, Nishimura K, Yamauchi J, Tanoue A (2010). Cytohesin-2/ARNO, through its interaction with focal adhesion adaptor protein paxillin, regulates preadipocyte migration via the downstream activation of Arf6. J Biol Chem 285, 24270–24281.
White DT, McShea KM, Attar MA, Santy LC (2010). GRASP and IPCEF promote ARF-to-Rac signaling and cell migration by coordinating the association of ARNO/cytohesin 2 with Dock180. Mol Biol Cell 21, 562–571.
Wong OG-W, Nitkunan T, Oinuma I, Zhou C, Blanc V, Brown RSD, Bott SRJ, Nariculam J, Box G, Munson P, *et al.* (2007). Plexin-B1 mutations in prostate cancer. Proc Natl Acad Sci USA 104, 19040–19045.
Wozniak MA, Kwong L, Chodniewicz D, Klemke RL, Keely PJ (2005). R-Ras controls membrane protrusion and cell migration through the spatial regulation of Rac and Rho. Mol Biol Cell 16, 84–96.
Wurtzel J, Kumar P, Goldfinger L (2012). Palmitoylation regulates vesicular trafficking of R-Ras to membrane ruffles and effects on ruffling and cell spreading. Small GTPases 3, 139–153.
Zhang Z, Vuori K, Wang H, Reed JC, Ruoslahti E (1996). Integrin activation by R-ras. Cell 85, 61–69.